System analysis of a diesel engine with VGT and EGR

Master's thesis
performed in **Vehicular Systems**

by
Thomas Johansson

Reg nr: LiTH-ISY-EX-LITH-ISY-EX–05-2005

9th October 2005

System analysis of a diesel engine with VGT and EGR

Master's thesis

performed in **Vehicular Systems**,
Dept. of Electrical Engineering
at **Linköpings universitet**

by **Thomas Johansson**

Reg nr: LiTH-ISY-EX-LITH-ISY-EX–05-2005

Supervisor: **Johan Wahlström**
Linköpings Universitet

Examiner: **Associate Professor Lars Eriksson**
Linköpings Universitet

Linköping, 9th October 2005

Avdelning, Institution
Division, Department

Vehicular Systems,
Dept. of Electrical Engineering
581 83 Linköping

Datum
Date

9th October 2005

Språk
Language
☐ Svenska/Swedish
☒ Engelska/English
☐ ________________

Rapporttyp
Report category
☐ Licentiatavhandling
☒ Examensarbete
☐ C-uppsats
☐ D-uppsats
☐ Övrig rapport
☐ ________________

ISBN
—

ISRN
LITH-ISY-EX-LITH-ISY-EX–05-2005

Serietitel och serienummer
Title of series, numbering

ISSN
—

URL för elektronisk version
http://www.vehicular.isy.liu.se
http://www.ep.liu.se/exjobb/isy/2005/LITH-ISY-EX–05/

Titel Systemanalys av en dieselmotor med VGT och EGR
Title System analysis of a diesel engine with VGT and EGR

Författare Thomas Johansson
Author

Sammanfattning
Abstract

To fulfil emission requirements specified by environment demands, such as Euro 4 and Euro 5, there is a need to utilize engines based on technologies such as Variable Turbine Geometry (VGT) and Exhaust Gas Recirculation (EGR). A model of an engine using VGT and EGR was created by Ph.D student Johan Wahlström at Linköping University. This thesis evaluates Wahlström's model and shows how it successfully describes the engine and its behaviour. The thesis also confirms theories about the occurrens of non.minimum phase behaviour in different transfer functions, e.g. from VGT signal to the mass flow through the compressor.

An interesting phenomenon when applying VGT and EGR is a nonlinearity leading to, for example, that the same pressure in the intake manifold can occur for two different VGT signals. Such phenomenon can cause problems when designing a control system. Furthermore, this nonlinearity also results in a replacement of the nonminimum phase behaviour with an overshoot when a large (above 80%) VGT control signal is used.

This thesis also provides a linearized model, which describes the engine satisfactory. The linearization results in transfer functions with two zeros and three poles, whose locations do not change much when varying engine speed and load (except at high load and low engine speed). This fact will most likely make it possible to utilize just a few different linearizations for all speeds and loads. However, altering VGT and EGR positions greatly affect the transfer functions. Thus, several linearizations are probably needed to cover all operating points.

When designing a future control system a good strategy is to utilize a decoupled system since the model has strong cross-connections. Another solution would be to apply multi dimensional control strategy, e.g. LQ-theory.

Nyckelord
Keywords VGT, EGR, diesel engine

Abstract

To fulfil emission requirements specified by environment demands, such as Euro 4 and Euro 5, there is a need to utilize engines based on technologies such as Variable Turbine Geometry (VGT) and Exhaust Gas Recirculation (EGR). A model of an engine using VGT and EGR was created by Ph.D student Johan Wahlström at Linköping University. This thesis evaluates Wahlström's model and shows how it successfully describes the engine and its behaviour. The thesis also confirms theories about the occurrens of non.minimum phase behaviour in different transfer functions, e.g. from VGT signal to the mass flow through the compressor.

An interesting phenomenon when applying VGT and EGR is a nonlinearity leading to, for example, that the same pressure in the intake manifold can occur for two different VGT signals. Such phenomenon can cause problems when designing a control system. Furthermore, this nonlinearity also results in a replacement of the nonminimum phase behaviour with an overshoot when a large (above 80%) VGT control signal is used.

This thesis also provides a linearized model, which describes the engine satisfactory. The linearization results in transfer functions with two zeros and three poles, whose locations do not change much when varying engine speed and load (except at high load and low engine speed). This fact will most likely make it possible to utilize just a few different linearizations for all speeds and loads. However, altering VGT and EGR positions greatly affect the transfer functions. Thus, several linearizations are probably needed to cover all operating points.

When designing a future control system a good strategy is to utilize a decoupled system since the model has strong cross-connections. Another solution would be to apply multi dimensional control strategy, e.g. LQ-theory.

Keywords: VGT, EGR, diesel engine

Acknowledgements

I would like to thank my supervisor PhD student Johan Wahlström at the division of Vehicular Systems, Dept. of Electrical Engineering, at Linköping University for his support during the work with my Master Thesis. Also my examiner, Associate Professor Lars Eriksson, shall have great thanks for his valuable suggestions and point of views. Furthermore I would like to mention PhD student Martin Enqvist at the Division of Automatic Control and Communication Systems at Linköping University for some valuable discussions in the area of control theory.

Finally I would like to thank my older brother for his guidance towards my M.Sc. degree in Applied Physics and Electrical Engineering. I owe you one!

Linköping, October 2005
Thomas Johansson

Contents

Abstract **v**

Acknowledgements **vii**

1 Introduction **2**
1.1 Background 2
1.2 Thesis outline 2
1.3 Method 3

2 Engine model **5**
2.1 Validation 7

3 Engine characteristics **9**
3.1 Nonlinearities 9
3.2 Modeling of VGT equilibrium point 14

4 Step response **17**
4.1 Step in VGT position 17
4.2 Step in EGR position 20
4.3 Time constants 22
4.4 Bode frequency response 26

5 Linearization **29**
5.1 Linearization 29
5.2 Poles and zeros 31
  5.2.1 Variation of operating point 33
5.3 Validation of linearization 35
5.4 Cancel out poles and zeros 36
5.5 Relative gain array 39

6 Conclusion **41**
6.1 The model 41
6.2 Nonlineareties 41
6.3 Linearization 42

6.4 Control strategy 42

A Validation **43**
A.1 25% load, 1200 rpm 43
A.2 75% load, 1200 rpm 47
A.3 50% load, 1500 rpm 51
A.4 25% load, 1900 rpm 55
A.5 75% load, 1900 rpm 59

B Nomenclature **63**

Chapter 1

Introduction

This master thesis is carried out at the division of Vehicular Systems at Linköping University.

1.1 Background

In the last years there has been a lot of attention on the emissions created by diesel engines. The emissions are not allowed to exceed limits specified by environment demands. The environment demands are getting harder for every year and to be able not to exceed these limits there is a need to use technologies such as Exhaust Gas Recirculation and Variable Geometry Turbine.

Variable Geometry Turbine, VGT, is used frequently in diesel engines since it provide a way to control the turbine maintaining good efficiency. The way to do this is to change the effective area of the turbine using vanes [4].

Exhaust Gas Recirculation, EGR, is a way to control the NO emissions by cooling a portion of the exhaust gas down and then transfer it back to the intake. The cycle-to-cycle variations will however increase when using EGR which could result in misfire [4].

1.2 Thesis outline

When using technologies such as Exhaust Gas Recirculation and Variable Geometry Turbine, there will be a change in characteristics of the engine from a traditional diesel engine. The characteristics of a diesel engine using EGR and VGT include phenomenons such as nonminimum phase behaviour and nonlinearities. This report will focus on such phenomenons and state when they occur and the reason for it. Analyzing the characteristics and the behaviour of the system is important for a sucessful design of a future controller. A linearization of the engine model will also be made and some basic ideas of the design of a control system will be discussed in the end of the report.

1.3 Method

All work in this report is built upon a model of a diesel engine created by Johan Wahlström at the division of Vehicular Systems at Linköping University. All theories are tested on this model and validated with measurements made with a Scania diesel engine. The model itself will not be presented in this report as it is showed and explained in [7]. All designations in the report are the same as in [7] and can found in Appendix B.

Chapter 2

Engine model

The engine investigated in this report is a diesel engine with Variable Geometry Turbine and Exhaust Gas Recirculation illustrated in fig. 2.1.

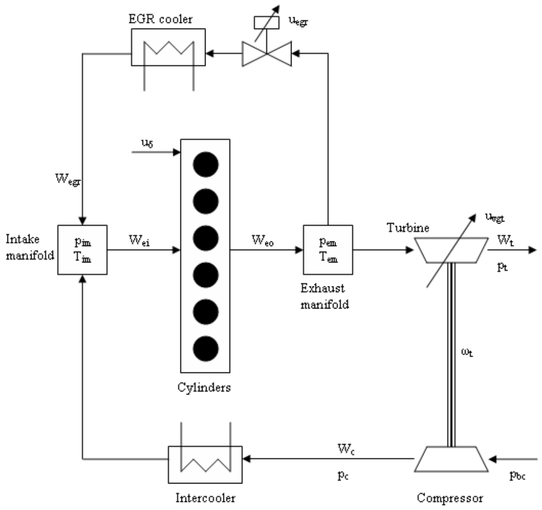

EGR cooler
u_{egr}
u_δ
W_{egr}
Intake manifold
p_{im}
T_{im}
W_{ei}
W_{eo}
p_{em}
T_{em}
Turbine
u_{vgt}
W_t
p_t
Exhaust manifold
ω_t
Cylinders
W_c
p_c
p_{bc}
Intercooler
Compressor

Figure 2.1: Illustration of the engine.

A useful model of the engine has been created by Johan Wahlström at Linköping University. The size or complexity of this model is crucial for the ability to use such a model in a control system because of the need in computer power. The model is therefore constructed with only five different states; intake- and exhaust manifold pressure, fraction of combustion parts in the intake- and exhaust manifold, and the turbine speed. The model can be written as [7]

$$\dot{x} = f(x, u) \tag{2.1}$$

$$y = h(x, u) \tag{2.2}$$

where u is the input vector

$$u = (u_\delta \, n_e \, u_{VGT} \, u_{EGR})^T \tag{2.3}$$

x is the state vector

$$x = (p_{im} \, p_{em} \, F_{im} \, F_{em} \, \omega_t)^T \tag{2.4}$$

and y is the output vector

$$y = (p_{im} \, p_{em} \, \omega_t \, W_c \, \lambda \, x_{EGR})^T \tag{2.5}$$

2.1 Validation

A number of simulations have been made for different loads and engine speeds to ensure the correctness of the model. By holding the VGT control signal constant and then apply a step in the EGR control signal, a good idea of the behaviour of the system can be obtained. The simulation is then carried out again but now with a constant EGR signal and a step in the VGT signal. By comparing the simulations with measurements for a number of different engine speeds and loads the model can be validated. All plots used for the validation are shown in Appendix A.

Comparison between simulations and measurements shows that the model describes the engine in a good way, especially if the main goal is to obtain a good way to describe the gas flow through the engine. It should however be said that the model of the torque produced by the engine, M_e, not seems to be a very good approximation for certain engine speeds and loads. Some examples of this shortcoming of the model can be seen in fig. A.10 and A.28. There are also some stationary errors, especially for the temperature models, when the engine is running at steady state. A thought was that this could be an explanation for the fact of the shortcoming of the engine torque model, and a compensation factor for the steady state error in the temperature models was tested. When analysing the model with this compensation factor it could be seen that the temperatures were described in a better way, but this affected the rest of the model in a bad way. A conclusion was therefore that this was not the main reason for the bad approximation of the torque produced by the engine. Also the effect of pumping losses has been investigated to see its influence on the shortcoming of the torque model but this effect has turned out to be too small to explain the bad behaviour of the model. The main goal at this stage is however to obtain a model that describes the gas flow through the engine in a good way, why the shortcoming of the torque model can be accepted at this stage. It could however be a good task for the future to construct a new model of the torque produced by the engine.

When it comes to the models of the temperatures the simulations seems to respond faster to a step in a control signal than the corresponding measurements. This can be explained with the fact that temperature measuring often is a slow process which results in a time displacement between real and measured temperatures.

A shortcoming in the validation process is the measurements. All measurements have been sampled at a rate of 1 Hz which is a too slow rate in comparison with the time constants of the system. A rule of thumb in modelling is to use a sample rate ten times faster than the time constants. If this rule of thumb should be followed, the sample rate should have been about 10 Hz or faster. The effect of this shortcoming can be seen when a step in a control signal occur which results in a slightly different behaviour of the model and the measurements.

Chapter 3

Engine characteristics

3.1 Nonlinearities

When the engine is running with a constant engine speed and load, an increase of the mass flow into the cylinders will take place if the VGT is almost fully opened and then is closed down a bit. The reason for this is a higher pressure in the exhaust manifold resulting in higher flow through the EGR valve and a higher turbine speed (and hence a higher flow through the compressor). However, if the VGT position is about 80% before the VGT position is closed down a bit, an decrease of the mass flow into the cylinders will instead take place. The reason for this is that some kind of equilibrium point[1] has been reached resulting in the opposite effect. Similar nonlinear behaviour also occurs for the intake manifold pressure, turbine speed and mass flow through the turbine. Fig. 3.1 shows a measurement where this nonlinear behaviour can be seen.

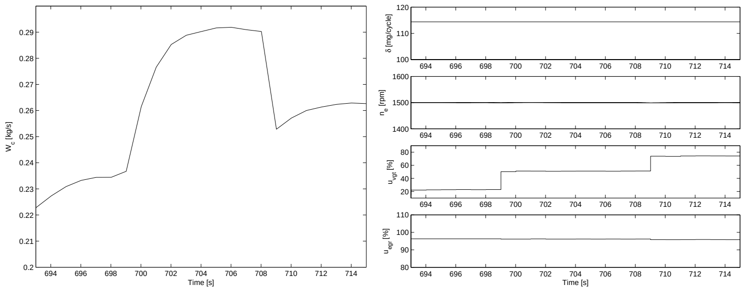

Figure 3.1: Measurement of nonlinear behaviour. **Left:** Mass flow through the compressor. **Right** Control signals.

---

[1] The point where the function has its maximum value.

These phenomena may for example result in big problems if the VGT signal is used to track and control the mass flow into the cylinders [3]. The problem becomes not easier of the fact that the equilibrium points for W_{ei}, p_{im}, ω_t and W_t varies for different positions of the EGR valve, engine speed and load. By just looking at the simulations in fig. 3.2-3.5, the relationship between EGR valve position and VGT equilibrium points seems to be approximately exponentially.

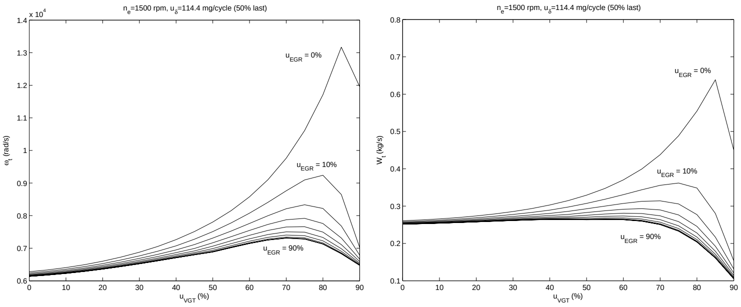

Figure 3.2: Simulated equilibrium points for the engine running at steady state. **Left:** Turbine speed for different VGT and EGR signals. **Right:** Mass flow through the turbine for different VGT and EGR signals.

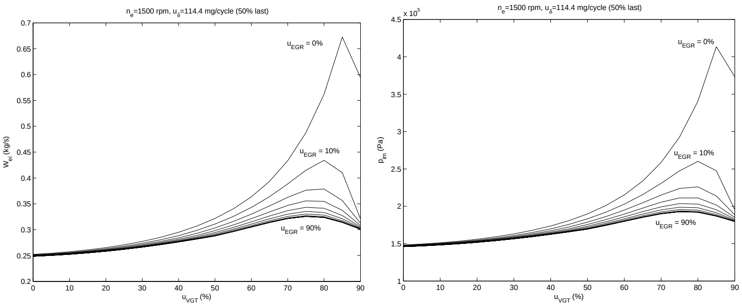

Figure 3.3: Simulated equilibrium points for the engine running at steady state. **Left:** Mass flow into the cylinders for different VGT and EGR signals. **Right:** Intake manifold pressure for different VGT and EGR signals.

When investigating the equilibrium points for the engine running at 1200 rpm and 75% load (fig. 3.4-3.5), it can be seen that the EGR valve positions does not seems to affect the system when a VGT position of about 50% or less is used. This is however just a shortcome of the model used to described the engine. The model is not constructed to handle backflow through the EGR valve which is what is happening as a result of higher pressure in the intake manifold than in the exhaust manifold. An improvement for the future is therefore to implement a backflow through the EGR valve.

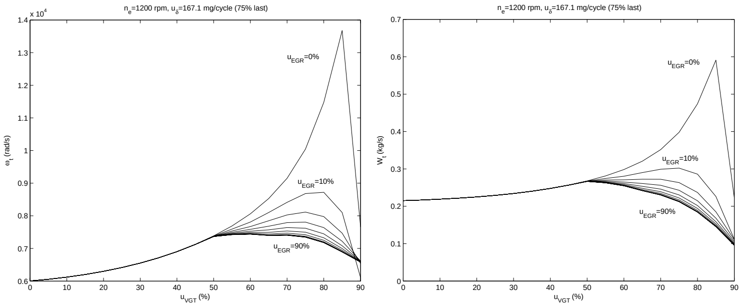

Figure 3.4: Simulated equilibrium points for the engine running at steady state. **Left:** Turbine speed for different VGT and EGR signals. **Right:** Mass flow through the turbine for different VGT and EGR signals.

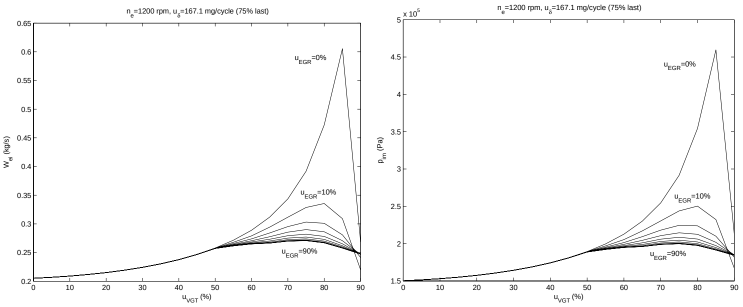

Figure 3.5: Simulated equilibrium points for the engine running at steady state. **Left:** Mass flow into the cylinders for different VGT and EGR signals. **Right:** Intake manifold pressure for different VGT and EGR signals.

Also different engine speeds and loads has an effect on the VGT equilibrium points. Lower load results in that the VGT equilibrium points occur when the VGT is more closed then when a higher load is used. The change of equilibrium point is however not very big and an idea could be to linearize this behaviour to achieve some grade of simplicity.

The effect of changing the engine speed is a bit fuzzier and a general rule, as in the case with the load, can not be given at this stage. The optimal solution for this problem would of course be to find an algebraic expression describing the physics resulting in this behaviour. There have been made several attempts to make a physical or mathematical explanation of why this phenomenon exists. A good solution has however not been found as the mathematical expression describing the engine are huge and complex. It seems however to be a good idea to assume steady state which results in

$$W_c + W_f - W_t = 0 \tag{3.1}$$

and then try to express the exhaust manifold pressure as a function of the control signals. It will however turn out that the exhaust manifold pressure also depends on the intake manifold pressure and the temperature in the exhaust manifold. The intake manifold pressure could probably in this case be approximated as $p_{im} = cp_{em}$ without loosing necessary information. The big problem has turned out to be the temperature in the exhaust manifold as this temperature also shows the same nonlinearities as the exhaust manifold pressure. The fact that the model of the temperature is not analytical and must be calculated through iterations makes this problem hard to solve. Instead of trying to solve the problem with the temperature, a suggestion for a solution in the future would be to investigate the effect on introducing some new states. Maybe this could make the whole problem a bit easier to solve. Introducing a new state will however make the model larger and less useful.

Fig. 3.6-3.7 shows the effect on the equilibrium point when changing operating point, i.e changing engine speed and load.

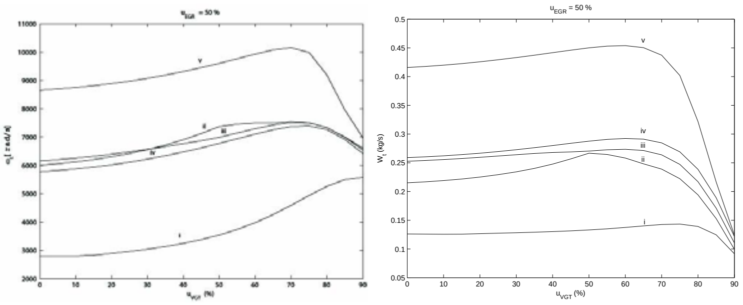

Figure 3.6: **i:** 1200 rpm, 25 % load, 50 % EGR. **ii:** 1200 rpm, 75 % load, 50 % EGR. **iii:** 1500 rpm, 50 % load, 50 % EGR. **iv:** 1900 rpm, 25 % load, 50 % EGR. **v:** 1900 rpm, 75 % load, 50 % EGR. **Left:** Turbine speed for different VGT signals. **Right:** Mass flow through the turbin.

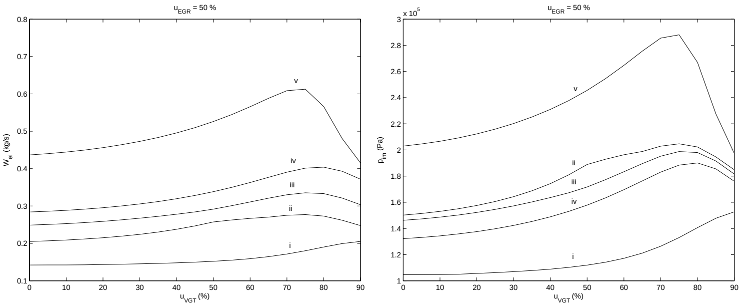

Figure 3.7: **i:** 1200 rpm, 25 % load, 50 % EGR. **ii:** 1200 rpm, 75 % load, 50 % EGR. **iii:** 1500 rpm, 50 % load, 50 % EGR. **iv:** 1900 rpm, 25 % load, 50 % EGR. **v:** 1900 rpm, 75 % load, 50 % EGR. **Left:** Mass flow into the cylinders for differnet VGT signals. **Right:** Intake manifold pressure for different VGT signals.

3.2 Modeling of VGT equilibrium point

As discussed in section 3.1 does the VGT equilibrium point, x_{VGT}, varies for different operating points. It could however be seen that the VGT equilibrium point decreases for increased engine speed, EGR valve position and engine load. The optimal solution to this problem would of course be to find an algebraic solution that describes the physics behind these phenomena. The model is though very complex and some parts are not analytical which makes this very difficult.

If there only is a need to have the possibility to track when the equilibrium point will occur, an easy solution is to model the equilibrium point as a black box model. This could for example be useful in a control system where it is more important to be able to tell when these phenomena will occur than why. A good model has turned out to be

$$x_{VGT} = c_1\sqrt{u_{EGR}} + c_2 u_\delta + c_3 n_e + c_4 n_e^2 + c_5 \tag{3.2}$$

where x_{VGT} is the VGT equilibrium point.

The least square method has been used to calculate the constants c_1-c_5 with the following results:

c_1=-11.4584·10^{-2}
c_2=-7.5446·10^{-2}
c_3=-64.8031·10^{-3}
c_4=-64.8031·10^{-6}
c_5=145.4841

These constants are valid for the VGT equilibrium point affecting the intake manifold pressure. Changing transfer function would of course change the constants c_1-c_5. The change of constants would however not be very big and the equilibrium point would still occur at about 80% VGT position. To avoid the problem with the VGT equilibrium point, a choice could be to limit the operating point to about 0-75% VGT position. The drawback would however be lower turbine speed and mass flows, i.e. the engine will perform less than its capacity.

Fig. 3.8 shows how the error in the VGT equilibrium point using eq. 3.2 depends on different inputs. The error in the VGT equilibrium point using the model described in eq. 3.2 seems to be about ±5 percent units. The size of the model error is though not very big and the model could therefore probably be used with success to track the VGT equilibrium point.

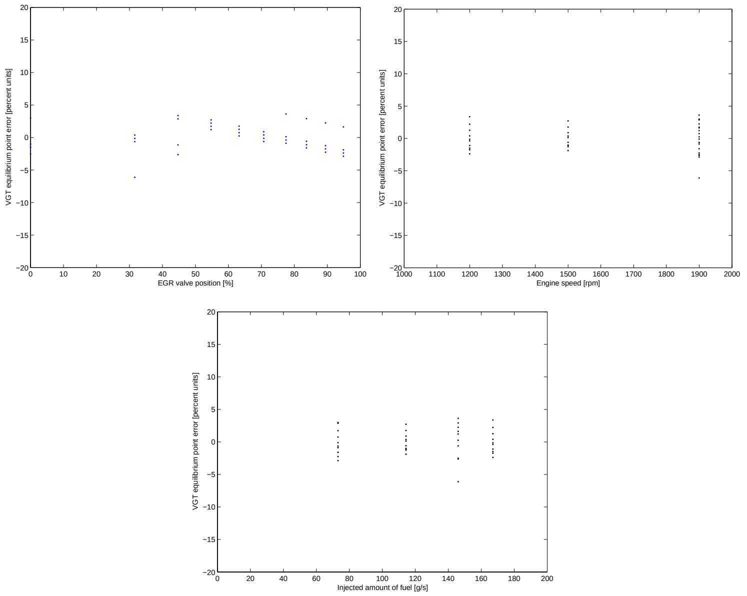

Figure 3.8: VGT equilibrium point error as a function of EGR valve position, engine speed and injected amount of fuel when using the model described by eq. 3.2

Chapter 4

Step response

4.1 Step in VGT position

When applying a closing step in the VGT control signal, the exhaust manifold pressure will start to increase. This results in a higher mass flow through the EGR and a higher intake manifold pressure.

Closing the VGT will also result in lower mass flows through both the turbine and the compressor in the beginning. But as a result of the increasing pressure in the exhaust manifold, these mass flows will eventually increase and after a while reach a state where the mass flows are higher than they were before the step in the VGT position took place. This is a typical behaviour for a nonminimum phase behaviour and is a result of zeros in the right half plane in the pole-zero map of the system. This nonminimum phase behaviour can be a problem if the mass flow through the turbine or the compressor is used as an input to control the system. By choosing another state as input for the control system, e.g. the intake manifold pressure, this problem can be avoided. Measuring another state may however result in a need for another type of sensor which may be expensive or not available and therefore not an option.

Fig. 4.1-4.4 shows the behaviour of the system for a step in the VGT control signal. Fig. 4.4 is particularly interesting as it shows the nonminimum behaviour for the mass flow through the turbine and the compressor.

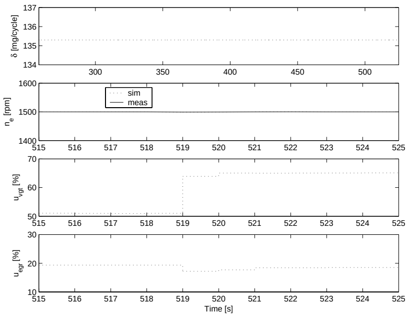

Figure 4.1: Control signals for a step in the VGT position.

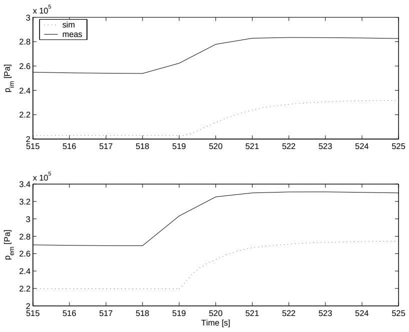

Figure 4.2: Comparison of measurements and model for a step in the VGT position. **Top:** Intake manifold pressure, p_{im}. **Bottom:** Exhaust manifold pressure, p_{em}.

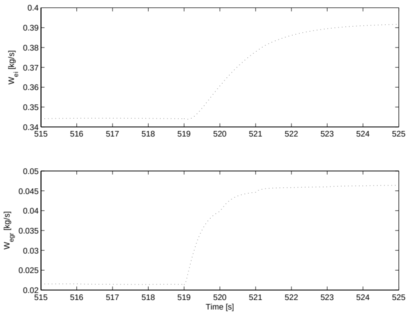

Figure 4.3: Simulations for a step in the VGT position. **Top:** Mass flow into the cylinders, W_{ei}. **Bottom:** Mass flow through the EGR, W_{EGR}.

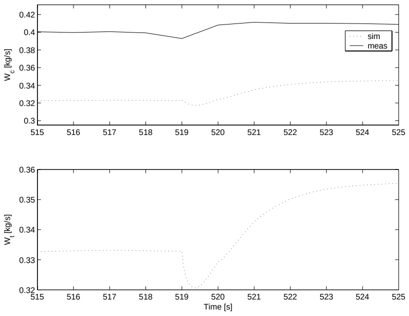

Figure 4.4: Comparison of measurements and model for a step in the VGT position. The appearance of the step response is characteristic for a nonminimum phase behaviour. **Top:** Mass flow through the compressor, W_c. **Bottom:** Mass flow through the turbine, W_t.

When applying a step in the VGT position after the equlibrium point has been reached (above 80% VGT), the nonminimum phase behaviour will no longer take place. The system will instead show overshoots. This can be explaind by the fact that when using a VGT position larger than the equilibrium point, an increase of the VGT position will have the opposite effect than when a VGT position less than the equilibrium point is used (see section 3.1). Fig. 4.5 shows the appearence of overshoots when a VGT step occur.

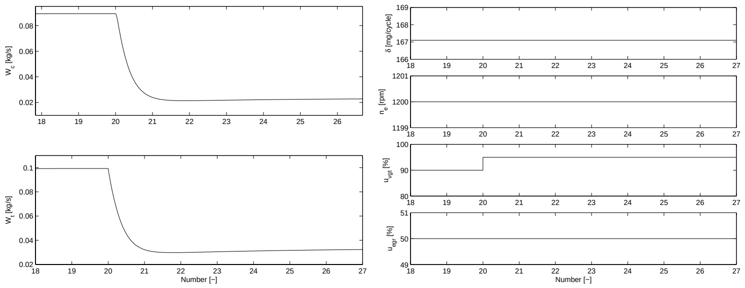

Figure 4.5: Simulations for a step in the VGT position. **Top-left:** Mass flow through the compressor. **Bottom-left:** Mass flow through the turbine. **Right:** Control signals.

4.2 Step in EGR position

If an instantaneous EGR valve opening occurs, there will be an increase of the mass flow through the EGR valve resulting in an increase of the intake manifold pressure. But higher mass flow through the EGR valve will result in lower mass flow through the turbine and eventually affect the intake manifold pressure in the opposite direction, i.e. a decrease of the pressure. This kind of behaviour is typical for a nonminimum phase system and may result in big difficulties if this signal is used as an input for a control signal. As in the case with the nonminimum phase behaviour for a change in the VGT position this could be solved by using a different signal as an input to a control signal. A change of signal may however result in a need for another type of sensor.

When comparing the measurements and the model it can be seen that the model seems to describe the engine in a good way. As fig. 4.6-4.9 shows there are small steady state errors, but at this stage this is not crucial as the essential thing is to obtain a good model of the dynamics of the gas flow through the engine. Fig. 4.7 and 4.8 is particularly interesting as it shows the nonminimun phase behaviour for the intake manifold pressure and the mass flow into the cylinders.

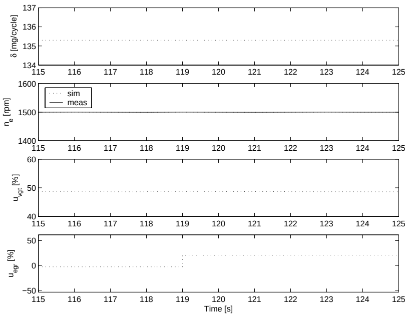

Figure 4.6: Control signals for a step in the EGR position.

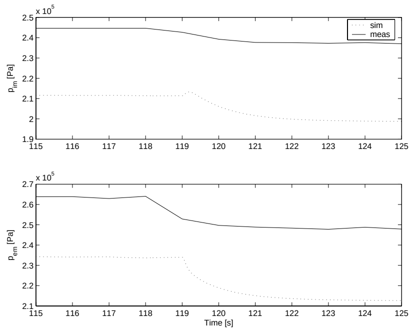

Figure 4.7: Comparison of measurements and model for a step in the EGR position. **Top:** Intake manifold pressure, p_{im}. **Bottom:** Exhaust manifold pressure, p_{em}.

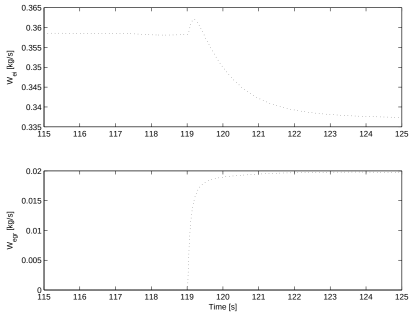

Figure 4.8: Simulations for a step in the EGR position. **Top:** Mass flow into the cylinders, W_{ei}. **Bottom:** Mass flow through the EGR, W_{EGR}.

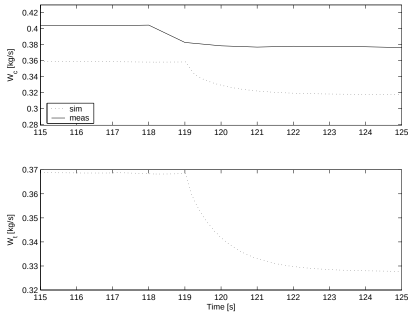

Figure 4.9: Comparison of measurements and model for a step in the EGR position. **Top:** Mass flow through the compressor, W_c. **Bottom:** Mass flow through the turbine, W_t.

4.3 Time constants

Previous section shows how the step responses differ for different transfer functions. This gives an idea of which transfer function that has the fastest response and can be used to give some explanation of the characteristics of the engine. By changing the engine speed and load and look at the step responses again, the influence of these two inputs can be seen. It shows clearly that the time constants for the different transfer functions changes significant when a different engine speed or load is used, i.e. the transfer functions varies for different operating points. Different time constants for different conditions will result in some problems when designing a controller for the system, i.e. there will probably be a need of different control systems for different operating points.

All time constants have been calculated through simulations. Verifying the constants has not been possible since the measured data has been sampled at a too low rate, in this case 1 Hz, in comparison to the size of the time constants. It could however be seen that the calculated time constants seems to be approximately correct.

Transfer function	Time constant	Transfer function	Time constant
$u_{VGT} \rightarrow W_c$	2.06 s	$u_{EGR} \rightarrow W_c$	1.20 s
$u_{VGT} \rightarrow \omega_t$	2.41 s	$u_{EGR} \rightarrow \omega_t$	2.27 s
$u_{VGT} \rightarrow \lambda$	2.16 s	$u_{EGR} \rightarrow \lambda$	1.95 s
$u_{VGT} \rightarrow x_{EGR}$	0.10 s	$u_{EGR} \rightarrow x_{EGR}$	0.29 s
$u_{VGT} \rightarrow F_{im}$	0.14 s	$u_{EGR} \rightarrow F_{im}$	0.89 s
$u_{VGT} \rightarrow p_{im}$	1.88 s	$u_{EGR} \rightarrow p_{im}$	2.11 s
$u_{VGT} \rightarrow p_{em}$	0.72 s	$u_{EGR} \rightarrow p_{em}$	1.15 s

Table 4.1: Time constants for 1200 rpm and 25 % load.

Transfer function	Time constant	Transfer function	Time constant
$u_{VGT} \rightarrow W_c$	0.21 s	$u_{EGR} \rightarrow W_c$	0.98 s
$u_{VGT} \rightarrow \omega_t$	1.54 s	$u_{EGR} \rightarrow \omega_t$	1.55 s
$u_{VGT} \rightarrow \lambda$	0.34 s	$u_{EGR} \rightarrow \lambda$	1.36 s
$u_{VGT} \rightarrow x_{EGR}$	0.24 s	$u_{EGR} \rightarrow x_{EGR}$	0.17 s
$u_{VGT} \rightarrow F_{im}$	0.42 s	$u_{EGR} \rightarrow F_{im}$	0.71 s
$u_{VGT} \rightarrow p_{im}$	1.18 s	$u_{EGR} \rightarrow p_{im}$	1.45 s
$u_{VGT} \rightarrow p_{em}$	0.31 s	$u_{EGR} \rightarrow p_{em}$	0.98 s

Table 4.2: Time constants for 1200 rpm and 75 % load.

Transfer function	Time constant	Transfer function	Time constant
$u_{VGT} \to W_c$	0.11 s	$u_{EGR} \to W_c$	0.91 s
$u_{VGT} \to \omega_t$	1.42 s	$u_{EGR} \to \omega_t$	1.42 s
$u_{VGT} \to \lambda$	1.35 s	$u_{EGR} \to \lambda$	1.30 s
$u_{VGT} \to x_{EGR}$	0.20 s	$u_{EGR} \to x_{EGR}$	0.15 s
$u_{VGT} \to F_{im}$	0.33 s	$u_{EGR} \to F_{im}$	0.72 s
$u_{VGT} \to p_{im}$	1.35 s	$u_{EGR} \to p_{im}$	1.34 s
$u_{VGT} \to p_{em}$	0.48 s	$u_{EGR} \to p_{em}$	0.96 s

Table 4.3: Time constants for 1500 rpm and 50 % load.

Transfer function	Time constant	Transfer function	Time constant
$u_{VGT} \to W_c$	0.10 s	$u_{EGR} \to W_c$	0.82 s
$u_{VGT} \to \omega_t$	1.19 s	$u_{EGR} \to \omega_t$	1.33 s
$u_{VGT} \to \lambda$	1.25 s	$u_{EGR} \to \lambda$	1.23 s
$u_{VGT} \to x_{EGR}$	0.22 s	$u_{EGR} \to x_{EGR}$	0.13 s
$u_{VGT} \to F_{im}$	0.28 s	$u_{EGR} \to F_{im}$	0.70 s
$u_{VGT} \to p_{im}$	1.13 s	$u_{EGR} \to p_{im}$	1.24 s
$u_{VGT} \to p_{em}$	0.51 s	$u_{EGR} \to p_{em}$	0.91 s

Table 4.4: Time constants for 1900 rpm and 25 % load.

Transfer function	Time constant	Transfer function	Time constant
$u_{VGT} \to W_c$	0.15 s	$u_{EGR} \to W_c$	0.85 s
$u_{VGT} \to \omega_t$	0.90 s	$u_{EGR} \to \omega_t$	1.29 s
$u_{VGT} \to \lambda$	0.93 s	$u_{EGR} \to \lambda$	1.21 s
$u_{VGT} \to x_{EGR}$	0.24 s	$u_{EGR} \to x_{EGR}$	0.11 s
$u_{VGT} \to F_{im}$	0.32 s	$u_{EGR} \to F_{im}$	0.73 s
$u_{VGT} \to p_{im}$	1.09 s	$u_{EGR} \to p_{im}$	1.22 s
$u_{VGT} \to p_{em}$	0.47 s	$u_{EGR} \to p_{em}$	0.85 s

Table 4.5: Time constants for 1900 rpm and 75 % load.

A step in EGR control signal results in a nonminimum phase behaviour for the intake manifold pressure. A reason for these phenomena can be seen by looking at fig. 4.10 and the time constants. The intake manifold pressure depends on the flow through the compressor which depends on the turbine speed. The turbine speed is a mechanical phenomenon which has slower dynamics than for example gas flows. The result will be that longer time passes by before the effect of lower/higher turbine speed can be seen in the intake manifold pressure. A step in VGT control signal will as shown earlier also result in a nonminimum phase behaviour for the flow through the compressor. The reason for this is the same as discussed for the EGR signal and the corresponding intake manifold pressure. Constructing an engine with a turbine that does not result in nonminimum phase behaviour is probably very hard as the mechanical dynamics are slow in comparison to the dynamics of the gas flows.

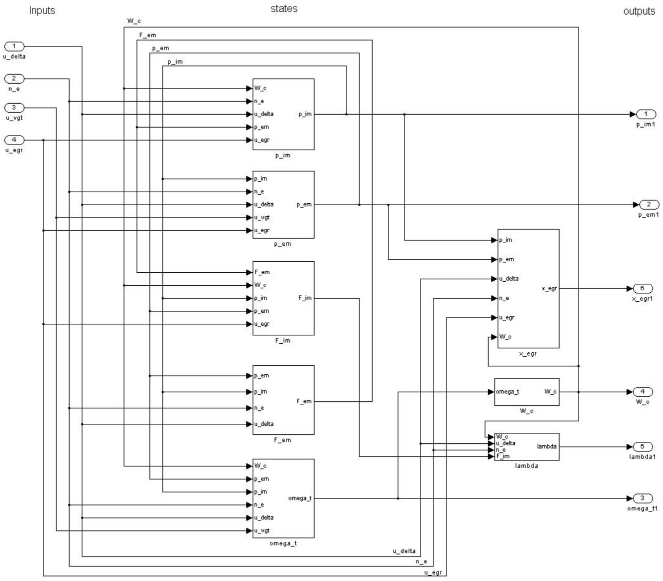
Inputs
states
outputs
1
u_delta
2
n_e
3
u_vgt
4
u_egr
W_c
F_em
p_em
p_im
W_c
n_e
u_delta
p_em
u_egr
p_im
p_im
p_im
n_e
u_delta
u_vgt
u_egr
p_em
p_em
F_em
W_c
p_im
p_em
u_egr
F_im
F_im
p_em
p_im
n_e
u_delta
F_em
F_em
W_c
p_em
p_im
n_e
u_delta
u_vgt
omega_t
omega_t
u_delta
n_e
u_egr
p_im
p_em
u_delta
n_e
u_egr
W_c
x_egr
x_egr
omega_t
W_c
W_c
W_c
u_delta
n_e
F_im
lambda
lambda
1
p_im1
2
p_em1
6
x_egr1
4
W_c
5
lambda1
3
omega_t1

Figure 4.10: The figure gives an overview of the flowchart of inputs, states and outputs.

4.4 Bode frequency response

By looking at bode frequency responses at different operating points, an idea of how much the input to output gain varies can be obtained. Fig. 4.11 shows the gain from the different inputs to the intake manifold pressure for different engine speeds and loads (constant VGT and EGR positions). As the figure shows the gains seems to be fairly constant over all operating points except the gain for the transfer function from the EGR input signal to the intake manifold pressure at high load and low engine speed. In chapter 5.2.1 will also the locations of the poles and zeros be investigated at different operating point. This in addition to the gain gives a good idea of which changes that occurs in the system when changing operating point. If it can be shown that only small changes occurs when changing operating point, there could probably be enough to use just one or a few different control systems for all engine speeds and loads except for high speed and low load.

Fig. 4.12 shows the gain from the different inputs to the intake manifold pressure for different VGT and EGR position (constant engine speed and load). In contrast to the previous case when changing only the engine speed and load, changing VGT and EGR position seems to affect the gain much more.

As a result from the bode frequency responses a suggestion is that the largest needs for different control systems for different operating points are when changing VGT and EGR positions. Changing the engine speed and load does not affect the gain in the same way.

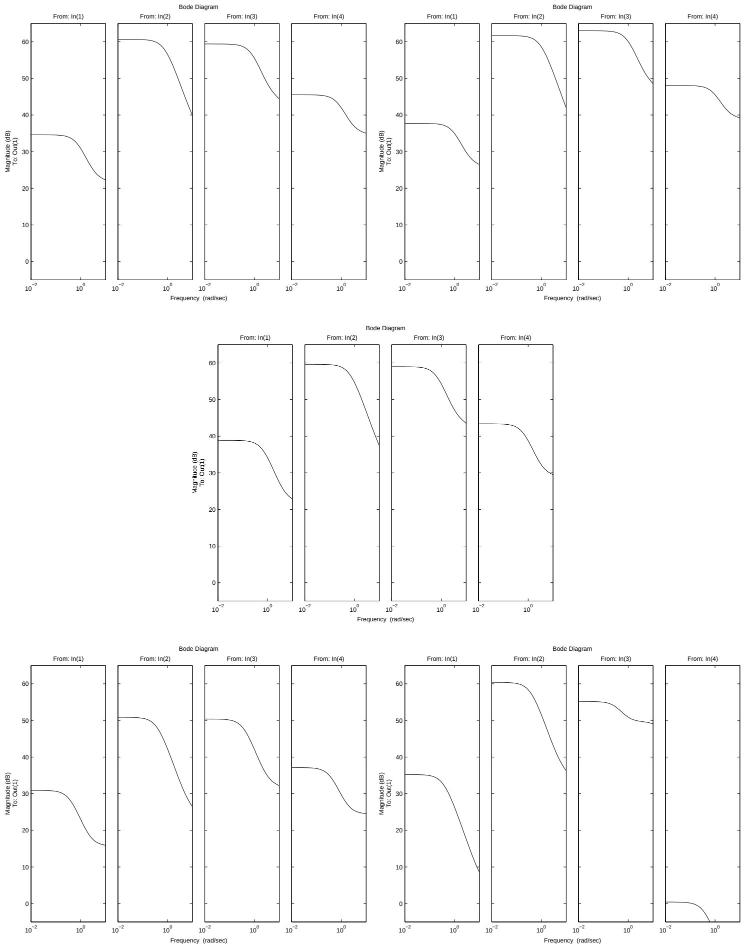

Figure 4.11: Bode frequency responses for the intake manifold pressure, p_{im}, at 50% VGT and EGR for different engine speeds and loads. There are four frequency responses for each operating point belonging to the inputs in the following order (from left to right): u_δ, n_e, u_{VGT} and u_{EGR}. **Top-left:** 1900 rpm, 25% load. **Top-right:** 1900 rpm, 75% load. **Middle:** 1500 rpm, 50% load. **Bottom-left:** 1200 rpm, 25% load. **Bottom-right:** 1200 rpm, 75% load.

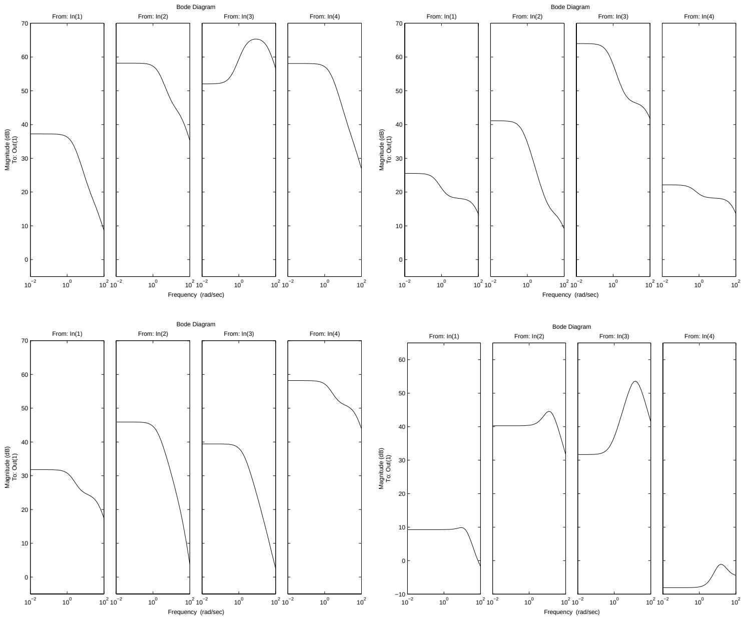

Figure 4.12: Bode frequency responses for the intake manifold pressure, p_{im}, at 1500 rpm and 50% load for different VGT and EGR positions. There are four frequency responses for each operating point beloning to the inputs in the following order (from left to right): u_{δ}, n_e, u_{VGT} and u_{EGR}. **Top-left:** 80% VGT and 20% EGR. **Top-right:** 80% VGT and 80% EGR. **Bottom-left:** 40% VGT and 20% EGR. **Bottom-right:** 40% VGT and 80% EGR.

Chapter 5

Linearization

5.1 Linearization

The model in previous chapter is nonlinear and can cause problems for a control system. Therefore is a linear approximation of the entire system desirable. To use the same linearization for different engine speeds, amount of fuel, EGR position and VGT position will however result in bad performance for the approximation. There are two different solutions for this problem. One way to go is to make a linearization of the model in real time. This has the advantage that the linearization for the actual operating point will always be correct. The drawback is that a huge amount of computer power is needed to been able to do this linearization in real time. The second solution is to make different linearizations for a number of different operating points in advanced, off-line, and then choose the linearization that is closest to the actual operating point. The advantage of this method is that the linearization does not have to be calculated during run time and there is therefore a save in computer power. The drawback is that if the operating point is not exactly the same as the linearization was made for, the linearization will not be entire correct but hopefully good enough for its purpose. This report has been focused on the last approach with a number of different linearizations calculated in advanced.

There are two major ways to make a linearization - numerical and algebraic. When using a algebraic approach, a Taylor series is created at the actual operating point. This approach is however not possible to perform at this specific system as the model is not analytical. A numerical aproach can instead be used where the solution is found through simulations.

According to [2] is

$$\dot{z} = Az + Bv \tag{5.1}$$
$$w = Cz + Dv \tag{5.2}$$

a linearization of

$$\dot{x} = f(x, u) \tag{5.3}$$
$$y = h(x, u) \tag{5.4}$$

in the equilibrium point $f(x_0, u_0) = 0$ where

$$z = x - x_0 \tag{5.5}$$
$$v = u - u_0 \tag{5.6}$$

The matrices A, B, C and D have the elements a_{ij}, b_{ij}, c_{ij} and d_{ij} given by

$$a_{ij} = \frac{\partial f_i}{\partial x_j}, \quad b_{ij} = \frac{\partial f_i}{\partial u_j}, \quad c_{ij} = \frac{\partial h_i}{\partial x_j}, \quad d_{ij} = \frac{\partial h_i}{\partial u_j} \tag{5.7}$$

An algebraic solution to eq. (5.7) does not exist as the model is not analytical [6] (the model of the exhaust gas temperature has to be solved with iterations). However, according to [5], eq. (5.7) can be numerically approximated by eq. (5.8)-(5.11).

$$a_{ij} = \frac{f_i(x_{01}, \ldots, x_{0j} + h, \ldots, x_{0n}, u_0) - f_i(x_0, u_0)}{h} \tag{5.8}$$
$$b_{ij} = \frac{f_i(x_0, u_{01}, \ldots, u_{0j} + h, \ldots, u_{0n}) - f_i(x_0, u_0)}{h} \tag{5.9}$$
$$c_{ij} = \frac{h_i(x_{01}, \ldots, x_{0j} + h, \ldots, x_{0n}, u_0) - h_i(x_0, u_0)}{h} \tag{5.10}$$
$$d_{ij} = \frac{h_i(x_0, u_{01}, \ldots, u_{0j} + h, \ldots, u_{0n}) - h_i(x_0, u_0)}{h} \tag{5.11}$$

5.2 Poles and zeros

As shown in previous chapters, the system has a nonminimum phase behaviour. Fig. 5.1 shows the pole-zero map for the transfer function from u_{EGR} to p_{im}. The pole-zero map for all transfer functions will not be shown in this chapter but it could however be said that all transfer functions have four zeros and five poles located in a similar way. As the map below shows there is a zero in the right half plane and this zero results in the non-minimum phase behaviour. The map also shows that two poles and zeros have almost the same location which would probably make it possible to cancel these poles and zeros to obtain a smaller and more useful model.

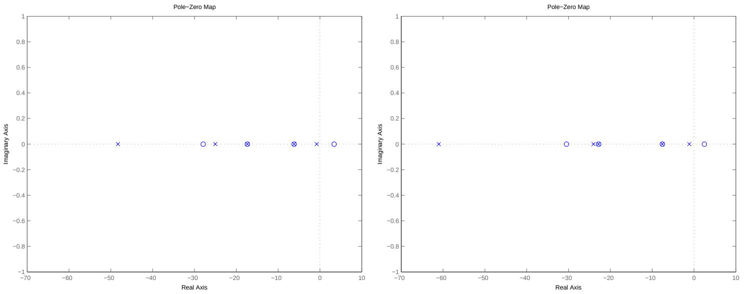

Figure 5.1: Pole-zero map for the transfer function from u_{EGR} to p_{im}. **Left:** Control signals: n_e=1500 rpm, u_δ=114.4 g/s, u_{VGT}=50 % u_{EGR}=30 %. **Right:** Control signals: n_e=1900 rpm, u_δ=146 g/s, u_{VGT}=30 % u_{EGR}=50 %.

The transfer functions from u_{EGR} to p_{im} can be written as

$$G_{u_{EGR},p_{im}}(s) = \frac{2984(s+27.90)(s-3.40)(s+17.34)(s+6.15)}{(s+48.30)(s+25.03)(s+0.77)(s+17.34)(s+6.15)} \tag{5.12}$$

at operating point n_e=1500 rpm, u_δ=114.4 g/s, u_{VGT}=50% and u_{EGR}=30%, and as

$$G_{u_{EGR},p_{im}}(s) = \frac{2859(s-2.49)(s+30.49)(s+7.55)(s+22.81)}{(s+61.02)(s+1.12)(s+24.02)(s+22.81)(s+7.55)} \tag{5.13}$$

at operating point n_e=1900 rpm, u_δ=146 g/s, u_{VGT}=30% and u_{EGR}=50%.

Fig. 5.2 shows the pole-zero map for the transfer function from u_{VGT} to W_c. Also this transfer function has a zero in the right half plane which can explain the non-minimum phase behaviour seen in fig. 4.4. As in the case with the transfer function from u_{EGR} to p_{im} two poles and zeros have almost the same location and could probably be removed to obtain a smaller model without loosing too much performance.

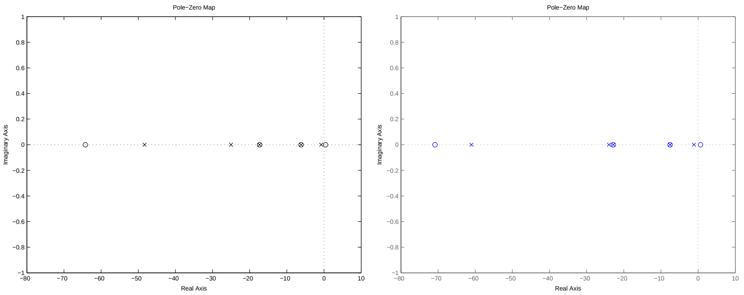

Figure 5.2: Pole-zero map for the trasfer function from u_{VGT} to W_c. **Left:** Control signals: n_e=1500 rpm, u_δ=114.4 g/s, u_{VGT}=50 % u_{EGR}=30 %. **Right:** Control signals: n_e=1900 rpm, u_δ=146 g/s, u_{VGT}=30 % u_{EGR}=50 %.

The transfer functions from u_{VGT} to W_c can be written as

$$G_{u_{VGT},W_c}(s) = \frac{-0.02066(s+64.22)(s-0.42)(s+6.15)(s+17.34)}{(s+48.30)(s+25.03)(s+0.77)(s+17.34)(s+6.15)} \tag{5.14}$$

at operating point n_e=1500 rpm, u_δ=114.4 g/s, u_{VGT}=50% and u_{EGR}=30%, and as

$$G_{u_{VGT},W_c}(s) = \frac{-0.01898(s+70.84)(s-0.62)(s+7.55)(s+22.81)}{(s+61.02)(s+1.12)(s+24.02)(s+22.81)(s+7.55)} \tag{5.15}$$

at operating point n_e=1900 rpm, u_δ=146 g/s, u_{VGT}=30% and u_{EGR}=50%.

Fig. 5.1-5.2 also shows that all poles are located in the left half plane and hence the system is stable according to [1].

As discussed in section 4.1, an increase of the VGT position beyond the equilibrium point will result in overshoot instead of nonminimum phase behavior. Fig. 5.3 shows the pole-zero map for some transfer function with a VGT position larger than the equilibrium point. As the figures shows there are no zeros located in the right half plane and the systems nonminimum phase behaviour does hence no longer exist.

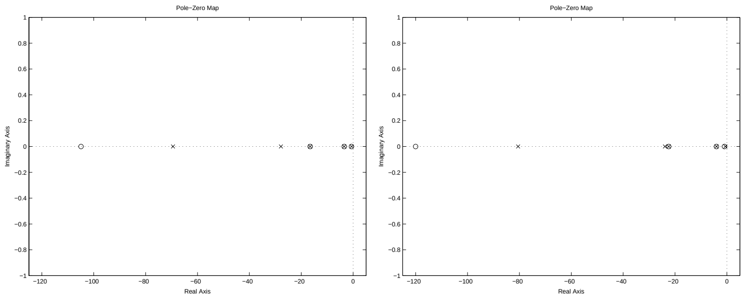

Figure 5.3: Pole-zero map for the trasfer function from u_{VGT} to W_c. **Left:** Control signals: n_e=1500 rpm, u_δ=114.4 g/s, u_{VGT}=85 % u_{EGR}=30 %. **Right:** Control signals: n_e=1900 rpm, u_δ=146 g/s, u_{VGT}=80 % u_{EGR}=50 %.

The transfer functions from u_{VGT} to W_c can be written as

$$G_{u_{VGT},W_c}(s) = \frac{0.0112(s+104.90)(s+0.67)(s+16.55)(s+3.44)}{(s+69.45)(s+27.84)(s+0.55)(s+16.55)(s+3.44)} \tag{5.16}$$

at operating point n_e=1500 rpm, u_δ=114.4 g/s, u_{VGT}=85% and u_{EGR}=30%, and as

$$G_{u_{VGT},W_c}(s) = \frac{0.0160(s+120.03)(s+0.96)(s+22.41)(s+4.04)}{(s+80.50)(s+23.88)(s+0.56)(s+22.41)(s+4.04)} \tag{5.17}$$

at operating point n_e=1900 rpm, u_δ=146 g/s, u_{VGT}=80% and u_{EGR}=50%.

5.2.1 Variation of operating point

When investigating the pole-zero map for different operating points it can be seen that the poles and zeros does not change their location much according to fig. 5.4. It could therefore be enough to use just a few different linearizations to achieve a linear model that is sufficient good to describe the engine. The crucial part of the operating points seams to be low engine speed and high load. The pole-zero map showing this operating point also have a pole located on the real axis at -771. This operating point was also the crucial part when investigating the bode frequency responses in chapter 4.4. All other operating points seams to have pole-zero maps that is not that different from each other.

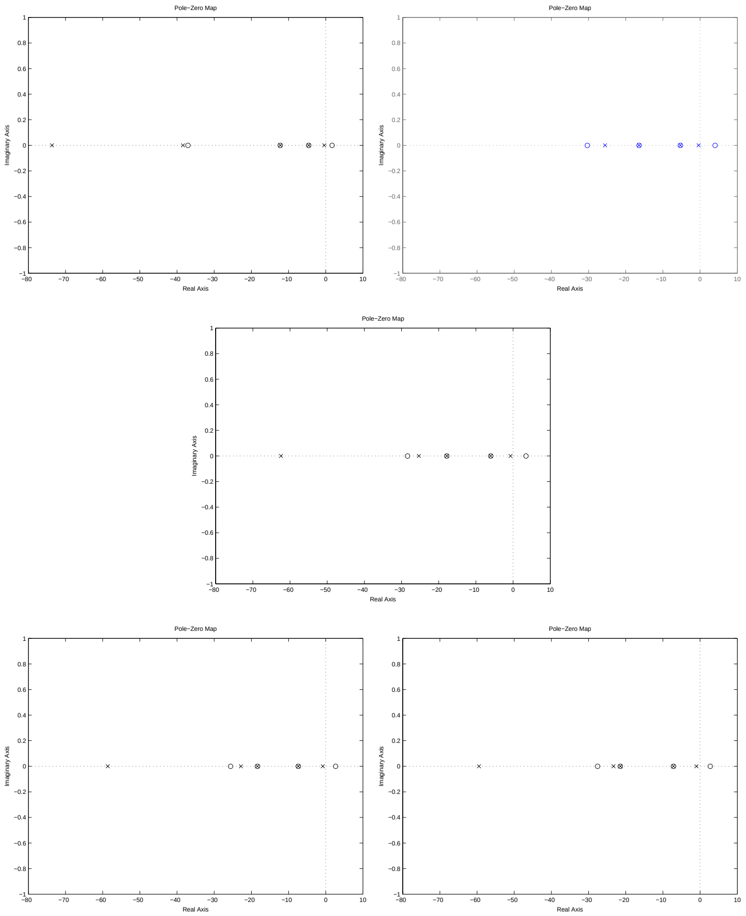

Figure 5.4: Pole-zero maps for the transfer function from u_{EGR} to p_{im} at different operating points. All pole-zero maps are generated with 50% EGR and 50% VGT. **Top-left:** Engine speed 1200 rpm and 25% load. **Top-right:** Engine speed 1200 rpm and 75% load. (there is also a pole not shown in figure located at -771) **Mid:** Engine speed 1500 rpm and 50% load.**Bottom-left:** Engine speed 1900 rpm and 25% load. **Bottom-right:** Engine speed 1900 rpm and 75% load.

5.3 Validation of linearization

To evaluate the performance of the linearization there is a need to make some kind of comparison with the non-linear model. This has been done by applying a step in one of the control signals and compare the step response from both the linearization and the non-linear model. As fig. 5.5-5.6 shows there is a small steady state error between the two models after the step in the control signal has occurred. This error is a result of a change in operating point. The linear model is designed to give a good approximation of the non-linear model at the conditions that are valid before the step take place. When the system reach steady state again after the step has occur the original condition is no longer valid and the hence there is a small steady state error. The dynamics of the liberalized model seems however to be correct and the linearization could therefore probably be acceptable.

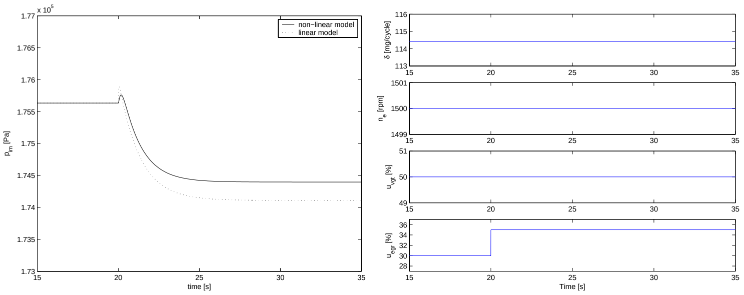

Figure 5.5: Step response for a change in EGR valve position. **Left:** Comparison of non-linear and linear model. **Right:** Control signals used for comparison of non-linear and linear model.

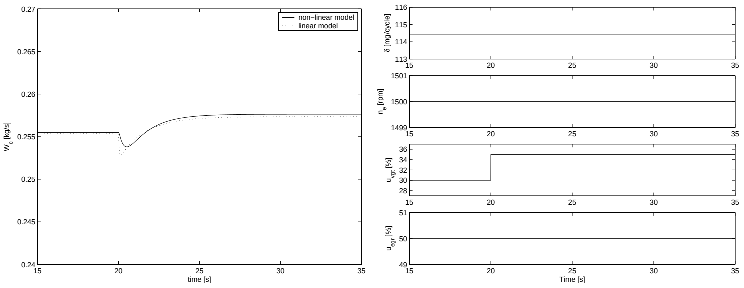

Figure 5.6: Step response for a change in VGT valve position. **Left:** Comparison of non-linear and linear model. **Right:** Control signals used for comparison of non-linear and linear model.

5.4 Cancel out poles and zeros

As discussed in previous section two poles and zeros have almost the same location. Removing these poles and zeros results in a smaller and probably more useful model. Fig. 5.7-5.8 shows the pole-zero maps with two poles and zeros removed.

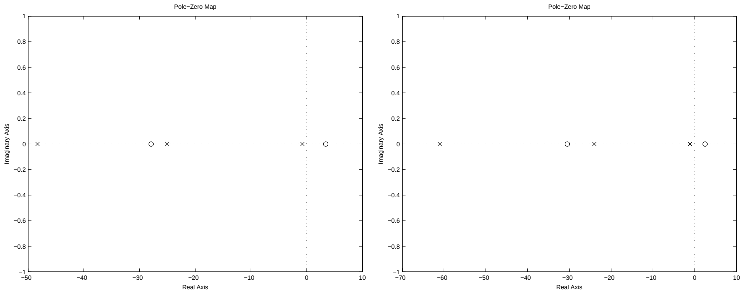

Figure 5.7: Pole-zero map for the transfer function from u_{EGR} to p_{im} with poles and zeros removed. **Left:** Control signals: n_e=1500 rpm, u_δ=114.4 g/s, u_{VGT}=50 % u_{EGR}=30 %. **Right:** Control signals: n_e=1900 rpm, u_δ=146 g/s, u_{VGT}=30 % u_{EGR}=50 %.

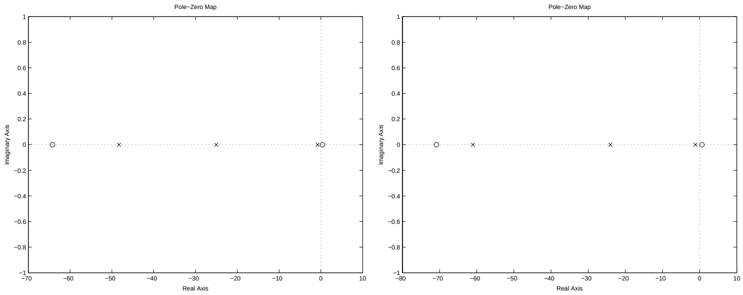

Figure 5.8: Pole-zero map for the trasfer function from u_{VGT} to W_c with poles and zeros removed. **Left:** Control signals: n_e=1500 rpm, u_δ=114.4 g/s, u_{VGT}=50 % u_{EGR}=30 %. **Right:** Control signals: n_e=1900 rpm, u_δ=146 g/s, u_{VGT}=30 % u_{EGR}=50 %.

To evaluate the effect of this simplification of the transfer functions same step response has been done as in previous section.

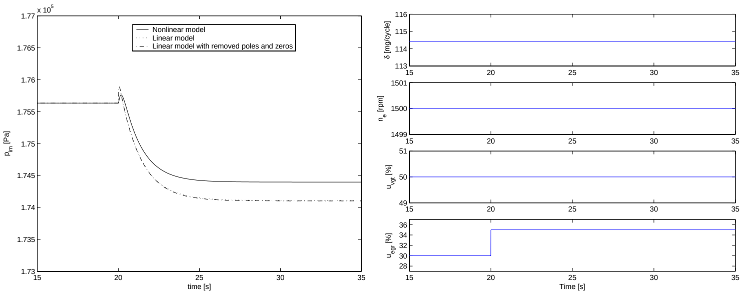

Figure 5.9: Step response for a change in EGR valve position. **Left:** Comparison of non-linear and different linear models. **Right:** Control signals used for comparison of non-linear and linear model.

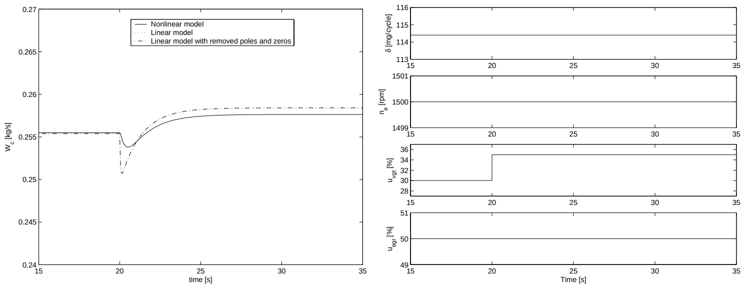

Figure 5.10: Step response for a change in VGT valve position. **Left:** Comparison of non-linear and different linear models. **Right:** Control signals used for comparison of non-linear and linear model.

Removing the poles and zeros located close to each other does not seams to affect the system in a major way as fig. 5.9-5.10 shows. This result shall not be surprisingly as the poles and zeros were located very close to each other. To remove these poles and zeros will therefore be a good idea to decrease the order of the system from five down to three. The final transfer functions can be written as

$$G_{u_{VGT},W_c}(s) = \frac{-0.02066(s+64.22)(s-0.42)}{(s+48.30)(s+25.03)(s+0.77)} \tag{5.18}$$

$$G_{u_{EGR},p_{im}}(s) = \frac{2984(s+27.90)(s-3.40)}{(s+48.30)(s+25.03)(s+0.77)} \tag{5.19}$$

at operating point n_e=1500 rpm, u_δ=114.4 g/s, u_{VGT}=50% and u_{EGR}=30%, and as

$$G_{u_{VGT},W_c}(s) = \frac{-0.01898(s+70.84)(s-0.62)}{(s+61.02)(s+1.12)(s+24.02)} \tag{5.20}$$

$$G_{u_{EGR},p_{im}}(s) = \frac{2859(s-2.49)(s+30.49)}{(s+61.02)(s+1.12)(s+24.02)} \tag{5.21}$$

at operating point n_e=1900 rpm, u_δ=146 g/s, u_{VGT}=30% and u_{EGR}=50%.

5.5 Relative gain array

A measurement of how coupled the system is can be obtained by calculating the relative gain array - RGA. The relative gain array for a quadratic matrix G is defined as [2]

$$RGA(G) = G. * (G^{-1})^T \tag{5.22}$$

The system in this case is however not quadratic (four inputs and six outputs) as eq. 5.22 demands. By changing the inverse in Eq. 5.22 to the pseudo inverse [2] the RGA formula will be

$$RGA(G) = G. * (G^{\dagger})^T \tag{5.23}$$

where the pseudo inverse is defined as

$$G^{\dagger} = (G^{*}G)^{-1}G^{*} \tag{5.24}$$

An optimal control solution would be to connect one input to one output (decentralized control strategy) and that changing the input would not affect the other outputs. One problem is obvious that the optimal solution needs a quadratic matrix, $G(s)$. This problem can be solved by just ignoring some of the inputs and outputs. In this case the biggest interest is to control λ and x_{EGR} using the control signals u_{VGT} and u_{EGR}. Ignoring all other inputs and outputs and calculating the relative gain array at 0 rad/s at operating point n_e=1500 rpm, u_δ=114.4 g/s, u_{VGT}=50% and u_{EGR}=50% gives the following result.

$$RGA(G(0)) = \begin{pmatrix} -0.0010 & 0.8240 \\ 0.0013 & 0.5730 \end{pmatrix} \tag{5.25}$$

with the elements corresponding to the inputs and outputs according to eq. 5.26-5.28.

$$Y(s) = G(s)U(s) \tag{5.26}$$

$$y(t) = (\lambda, x_{EGR})^T \tag{5.27}$$

$$u(t) = (u_{VGT}, u_{EGR})^T \tag{5.28}$$

When an element in the RGA matrix is close to one there is an indication that the corresponding input-output pair has a strong connection. When an element is not close to one should the output not be controlled by the corresponding input. The last statement is especially valid when the corresponding

RGA element has a negative value. If a decentralized control strategy has to be used, the best way is probably to make the connection in the following way.

$u_{VGT} \rightarrow x_{EGR}$
$u_{EGR} \rightarrow \lambda$

As eq. 5.25 shows it seems to be hard to use a decentralized control strategy in this case (the performance would probably not be very good). A better solution would be to use a decoupled control strategy where a new transfer function, $\tilde{G}(s)$, is created [2].

$$\tilde{G}(s) = W_2(s)G(s)W_1(s) \tag{5.29}$$

By choosing W_1 and W_2 in a good way, the new transfer function could have a RGA close to the unit matrix. Such a system could probably be controlled with one PID-controller connected to each input-output pair. Another solution to the controller problem would be to use a multi dimensional control strategy, e.g. LQ-theory.

Chapter 6

Conclusion

6.1 The model

The model presented in this thesis has turned out to describe the engine with satisfaction, especially if the gas flow through the engine is the most important part. The model successfully describes all known phenomenons such as nonlinearities and nonminimum phase behaviour. It should however be said that the submodel describing the torque produced by the engine demonstrates some model errors in a few operating points. Some of these errors can be explained by pumping losses, but not all. A suggestion for future work is therefore to make modifications to this submodel in order to obtain an even better overall model.

6.2 Nonlineareties

When suddenly opening up an almost closed VGT, an increase of the mass flow into the cylinders will occur. The same thing also occurs if the VGT suddenly goes from an almost fully opened state to a more closed state. Similar nonlinear behaviour is also observed for intake- and exhaust manifold pressure, turbine speed, and mass flows. The reason for this is still unknown since analyzing the physics and mathematics behind this phenomenon is a very demanding task. The best way to achieve a first explanation seems to be assuming steady state, W_c + W_f - W_t = 0, and try to express the exhaust manifold pressure as a function of only the four inputs (no states or other outputs). It has however turned out that exhaust manifold temperature has an influence on exhaust manifold pressure and that the temperature has to be solved through iterations. An early approach was to approximate the temperature with a constant, as its change is relatively small. However, this is not a good idea since the temperature shows the same nonlinearities as the exhaust manifold pressure. A suggestion for the future is therefore to try to find an analytical model of the exhaust manifold temperature, or introducing new states that makes this problem easier to solve. Introducing new states makes however the model larger and less useful.

6.3 Linearization

A linearization of the nonlinear system can with advantage be made numerically since the model is complex and includes a temperature factor that has to be calculated through iterations. Studying the pole-zero map of the linearized system reveal two poles and zeros located very close to each other. Removing these poles and zeros results in transfer functions with three poles and two zeros without loosing too much performance. The transfer functions from u_{VGT} to W_c also have a zero in the right half plane leading to a nonminimum phase behaviour when a u_{VGT} control signal less than the equilibrium point is used. The zero in the right half plane will however move into the left half plane when a u_{VGT} control signal bigger than the equilibrium is used. As a result of this the nonminimum phase behaviour is replaced by an overshoot.

When analysing the gain and pole-zero maps for the transfer functions, it can be observed that changing engine speed and load does not affect the transfer function very much, except when running the engine at high load and low engine speed. Because of this there is probably only a need for a few different linearizations covering all engine speeds and loads. However, changing VGT and EGR position greatly affects the transfer functions. Thus it is a greater need for several linearizations when changing EGR and VGT position.

6.4 Control strategy

By calculating the Relative Gain Array, RGA, it is clear that trying to connect one input to one output (dezentrelized control strategy) and achive good control opportunities is probably not possible. The first problem is that the model contains more outputs than inputs (six outputs and four inputs). This could however be solved by just ignoring four of the outputs and two of the inputs, i.e by just using u_{VGT}, u_{EGR}, λ and x_{EGR}. A greater problem is the fact that the system shows strong cross-connections. A better control strategy is to utilize a decoupled system or to apply a multi dimensional control strategy, e.g. LQ-theory.

Appendix A

Validation

A.1 25% load, 1200 rpm

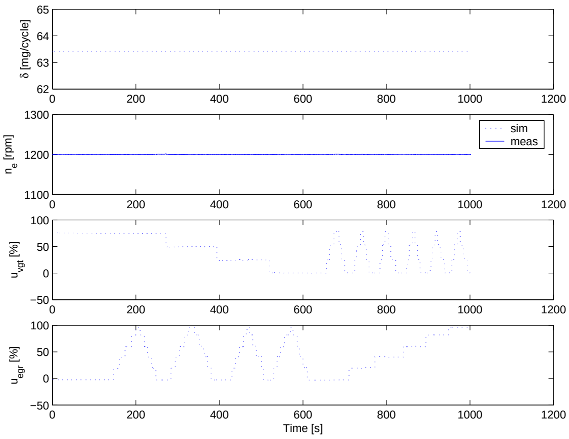

Figure A.1: Control signals.

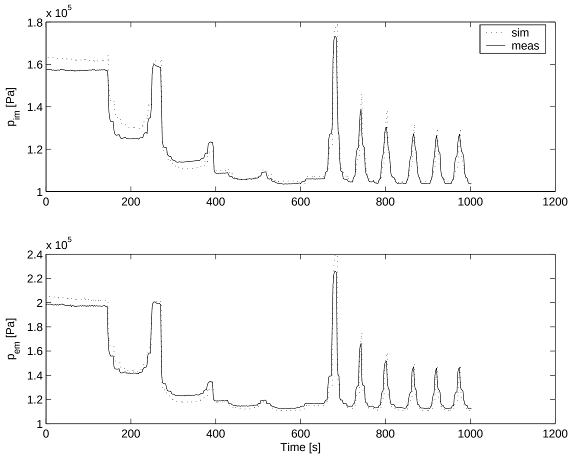

Figure A.2: Comparison of model and measurements. **Top:** Intake manifold pressure, p_{im}. **Bottom:** Exhaust manifold pressure, p_{em}.

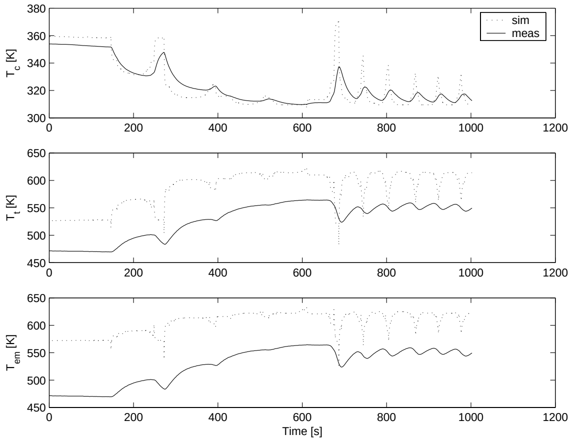

Figure A.3: Comparison of model and measurements. **Top:** Intake manifold temperature, T_{im}. **Middle:** Turbine temperature, T_t. **Bottom:** Exhaust manifold temperature, T_{em}.

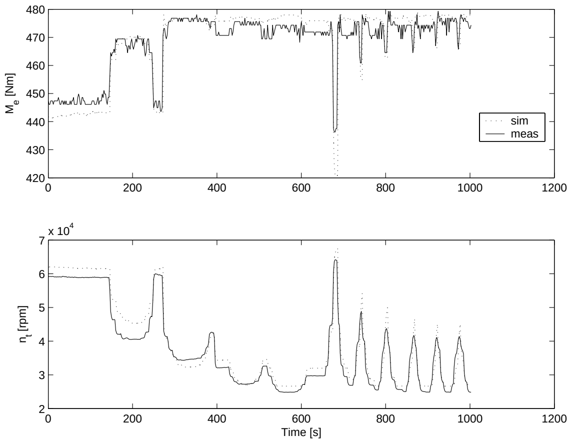

Figure A.4: Comparison of model and measurements. **Top:** Torque produced by the engine, M_e. **Bottom:** Turbine speed, n_t.

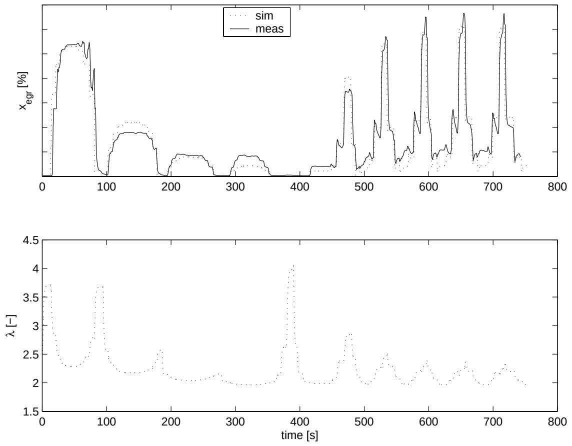

Figure A.5: **Top:** Comparison of model and measurements for fraction of EGR, x_{EGR}, in the intake manifold. **Bottom:** Model of the Air- to-fuel equivalence ratio, λ.

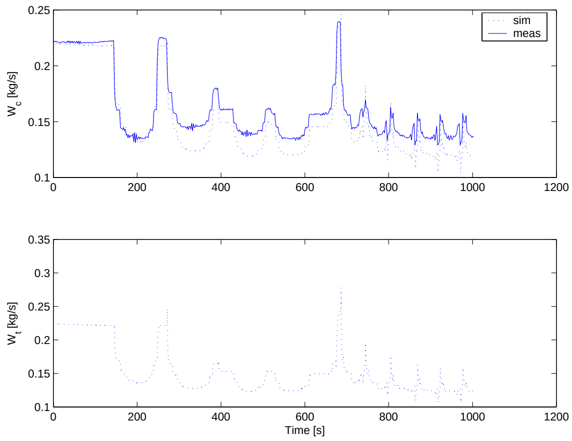

Figure A.6: Comparison of model and measurements. **Top:** Mass flow through the compressor, W_c. **Bottom:** Mass flow through the turbine, W_t.

A.2 75% load, 1200 rpm

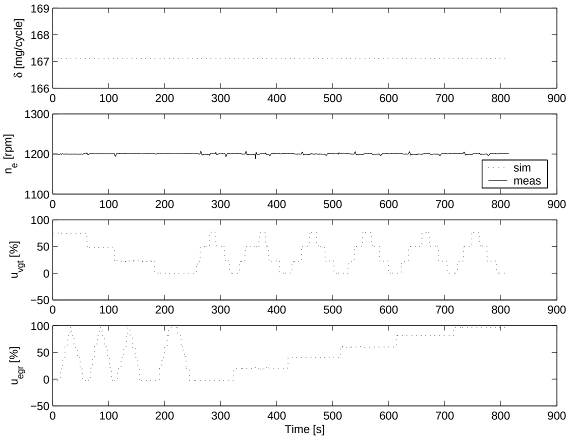

Figure A.7: Control signals.

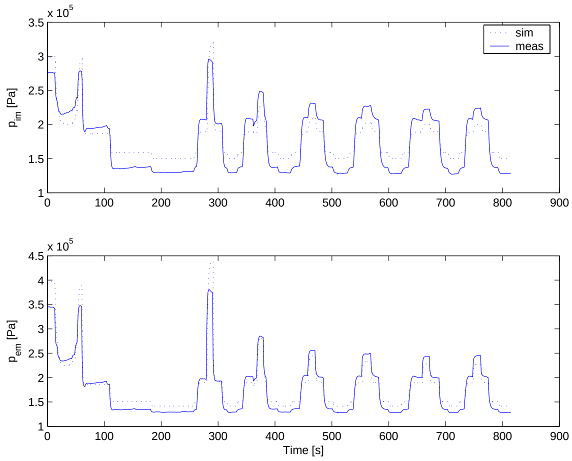

Figure A.8: Comparison of model and measurements. **Top:** Intake manifold pressure, p_{im}. **Bottom:** Exhaust manifold pressure, p_{em}.

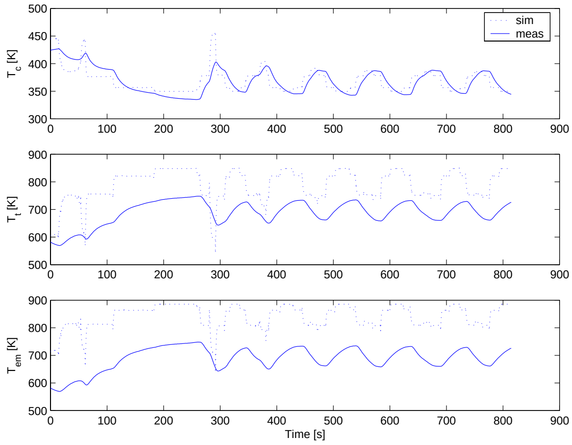

Figure A.9: Comparison of model and measurements. **Top:** Intake manifold temperature, T_{im}. **Middle:** Turbine temperature, T_t. **Bottom:** Exhaust manifold temperature, T_{em}.

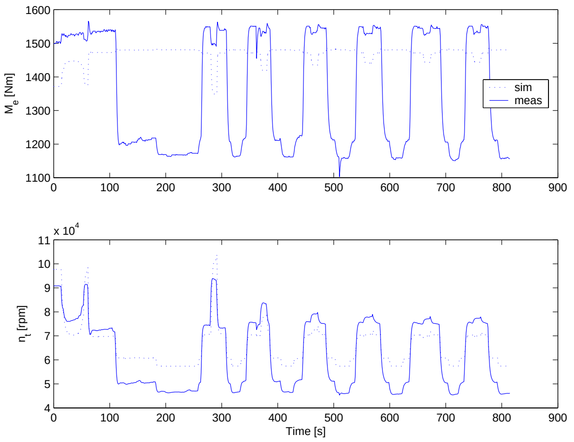

Figure A.10: Comparison of model and measurements. **Top:** Torque produced by the engine, M_e. **Bottom:** Turbine speed, n_t.

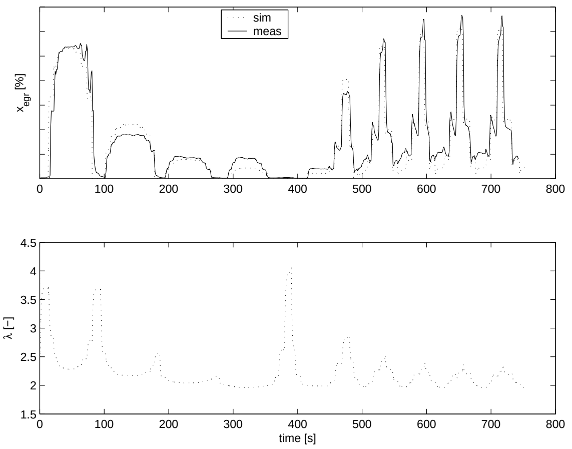

Figure A.11: **Top:** Comparison of model and measurements for fraction of EGR, x_{EGR}, in the intake manifold. **Bottom:** Model of the Air- to-fuel equivalence ratio, λ.

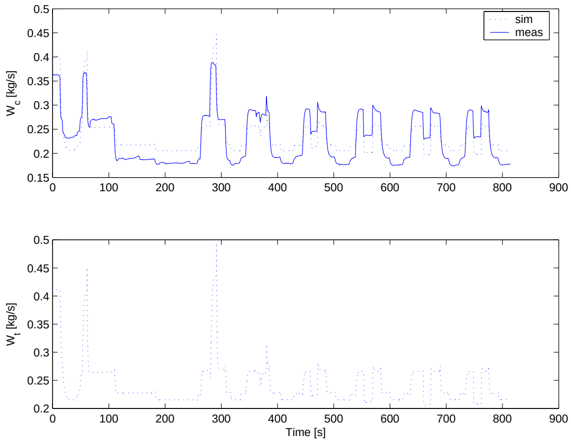

Figure A.12: Comparison of model and measurements. **Top:** Mass flow through the compressor, W_c. **Bottom:** Mass flow through the turbine, W_t.

A.3 50% load, 1500 rpm

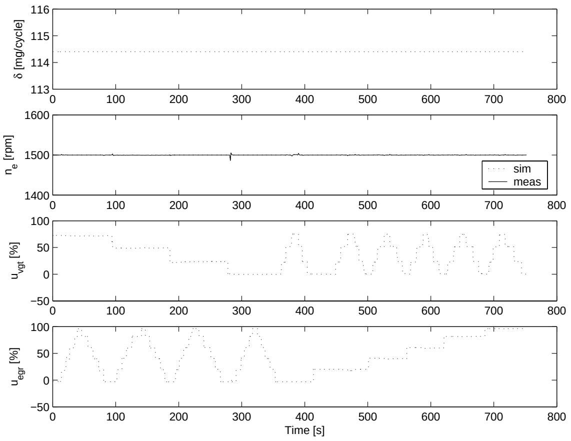

Figure A.13: Control signals.

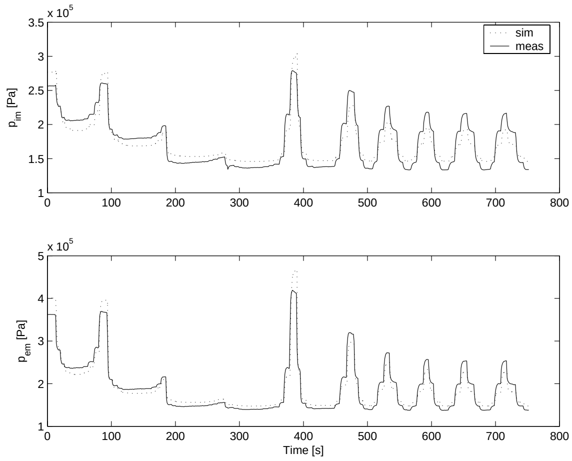

Figure A.14: Comparison of model and measurements. **Top:** Intake manifold pressure, p_{im}. **Bottom:** Exhaust manifold pressure, p_{em}.

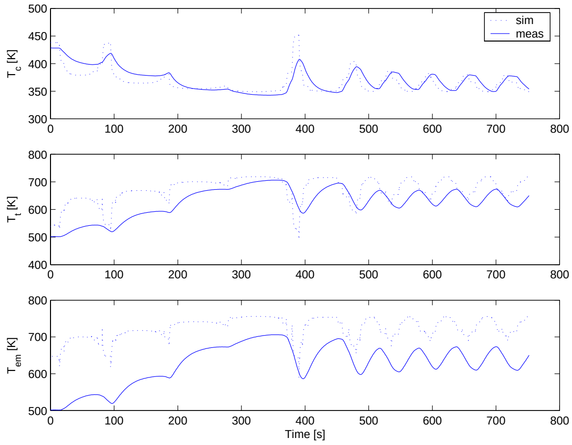

Figure A.15: Comparison of model and measurements. **Top:** Intake manifold temperature, T_{im}. **Middle:** Turbine temperature, T_t. **Bottom:** Exhaust manifold temperature, T_{em}.

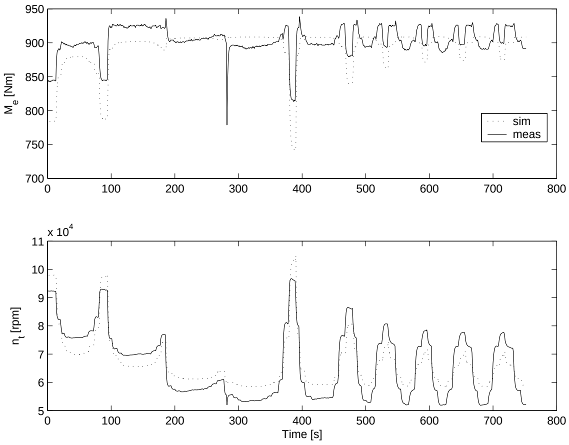

Figure A.16: Comparison of model and measurements. **Top:** Torque produced by the engine, M_e. **Bottom:** Turbine speed, n_t.

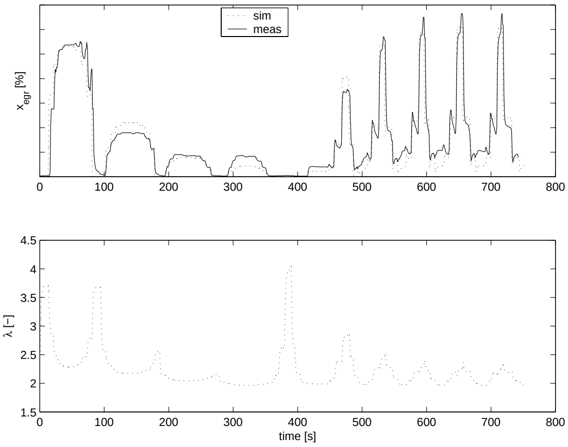

Figure A.17: **Top:** Comparison of model and measurements for fraction of EGR, x_{EGR}, in the intake manifold. **Bottom:** Model of the Air- to-fuel equivalence ratio, λ.

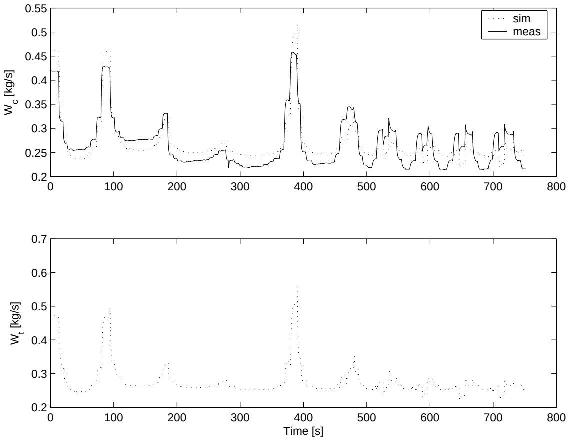

Figure A.18: Comparison of model and measurements. **Top:** Mass flow through the compressor, W_c. **Bottom:** Mass flow through the turbine, W_t.

A.4 25% load, 1900 rpm

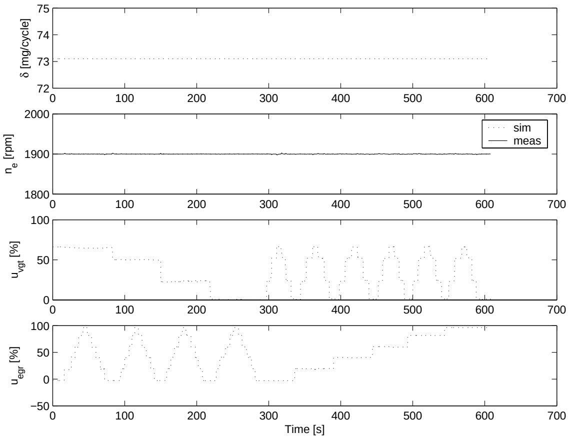

Figure A.19: Control signals.

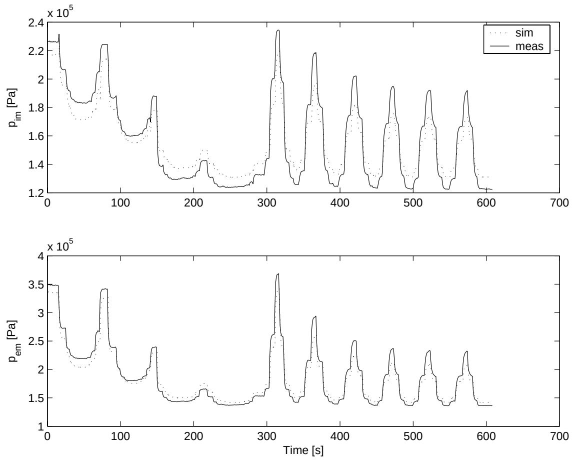

Figure A.20: Comparison of model and measurements. **Top:** Intake manifold pressure, p_{im}. **Bottom:** Exhaust manifold pressure, p_{em}.

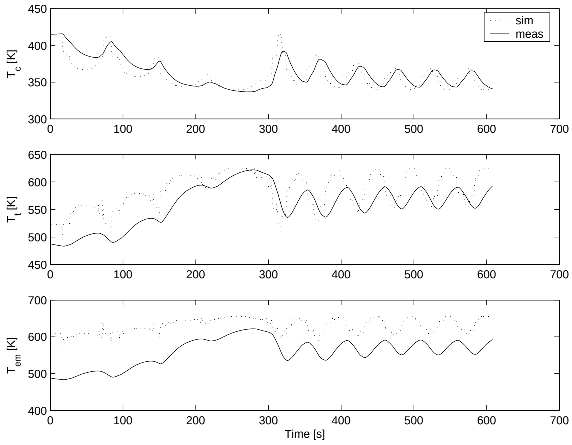

Figure A.21: Comparison of model and measurements. **Top:** Intake manifold temperature, T_{im}. **Middle:** Turbine temperature, T_t. **Bottom:** Exhaust manifold temperature, T_{em}.

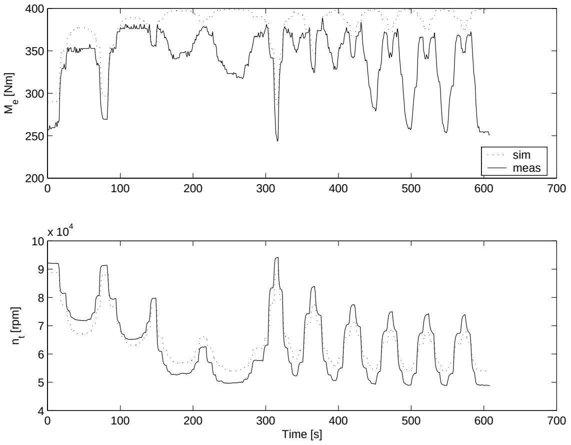

Figure A.22: Comparison of model and measurements. **Top:** Torque produced by the engine, M_e. **Bottom:** Turbine speed, n_t.

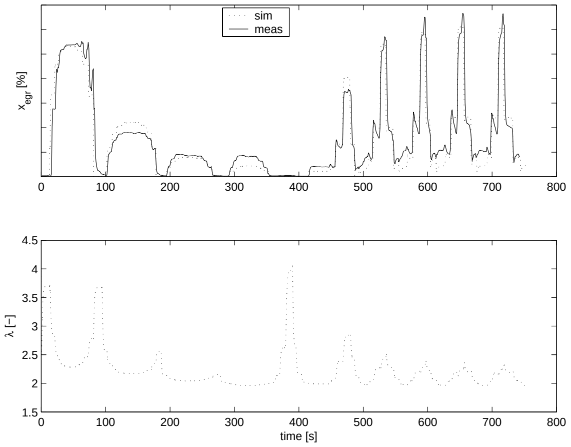

Figure A.23: **Top:** Simulation of fraction of EGR, x_{EGR}, in the intake manifold. **Bottom:** Model of the Air- to-fuel equivalence ratio, λ.

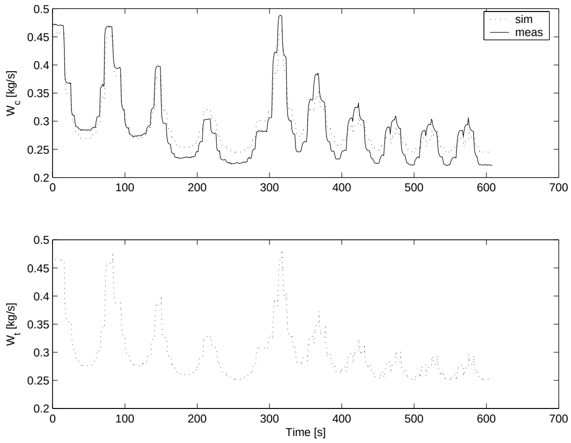

Figure A.24: Comparison of model and measurements. **Top:** Mass flow through the compressor, W_c. **Bottom:** Mass flow through the turbine, W_t.

A.5 75% load, 1900 rpm

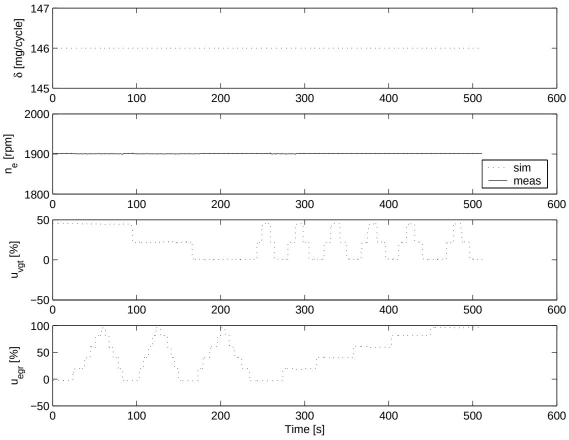

Figure A.25: Control signals.

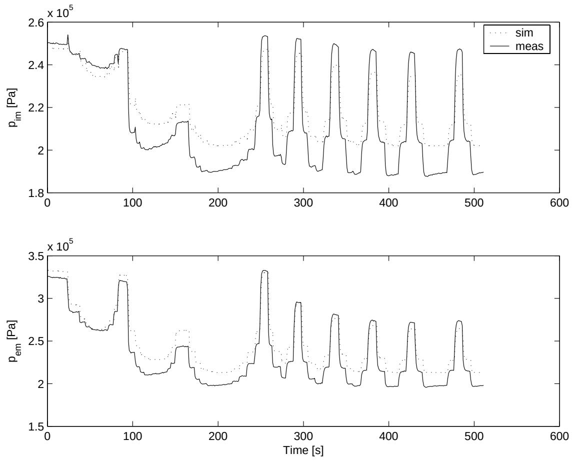

Figure A.26: Comparison of model and measurements. **Top:** Intake manifold pressure, p_{im}. **Bottom:** Exhaust manifold pressure, p_{em}.

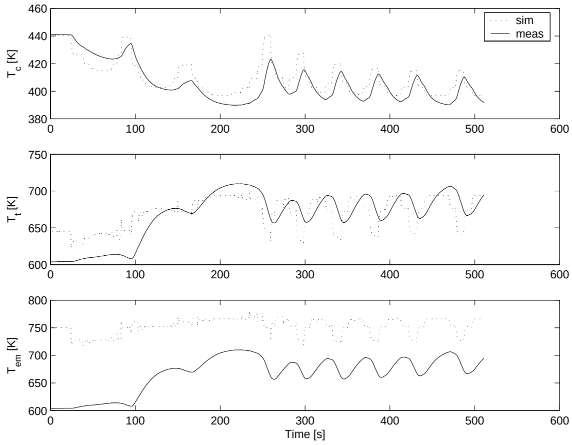

Figure A.27: Comparison of model and measurements. **Top:** Intake manifold temperature, T_{im}. **Middle:** Turbine temperature, T_t. **Bottom:** Exhaust manifold temperature, T_{em}.

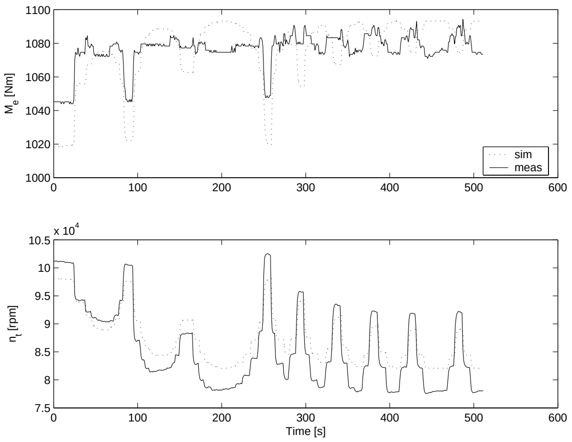

Figure A.28: Comparison of model and measurements. **Top:** Torque produced by the engine, M_e. **Bottom:** Turbine speed, n_t.

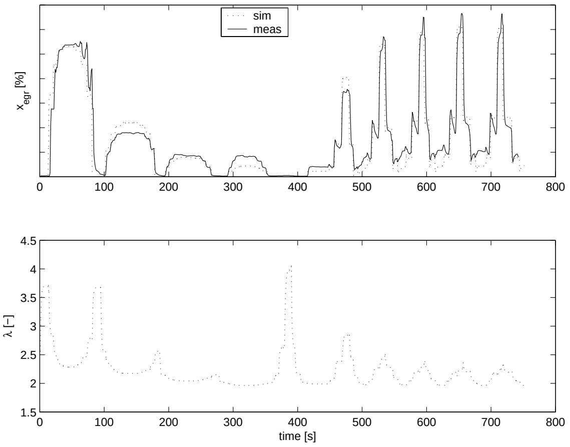

Figure A.29: **Top:** Comparison of model and measurements for fraction of EGR, x_{EGR}, in the intake manifold. **Bottom:** Model of the Air- to-fuel equivalence ratio, λ.

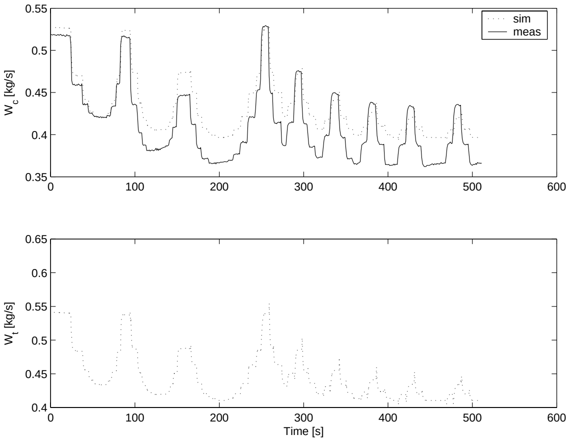

Figure A.30: Comparison of model and measurements. **Top:** Mass flow through the compressor, W_c. **Bottom:** Mass flow through the turbine, W_t.

Appendix B

Nomenclature

Variable	**Unit**	**Explanation**
F_{im}	-	Fraction of combustion products in the intake manifold
F_{em}	-	Fraction of combustion products in the exhaust manifold
M_e	Nm	Torque produced by the engine
n_e	rpm	Engine speed
n_t	rpm	Turbine speed
p_{em}	Pa	Exhaust manifold pressure
p_{im}	Pa	Intake manifold pressure
T_{em}	K	Exhaust manifold temperature
T_{im}	K	Intake manifold tempersture
T_t	K	Turbine temperature
u_δ	mg/cycle	Injected amount of fuel.
u_{EGR}	%	EGR control signal. 100 - open, 0 - closed
u_{VGT}	%	VGT control signal. 0 - open, 100 - closed
W_c	kg/s	Mass flow through the compressor
W_{ei}	kg/s	Mass flow into the cylinders
W_f	kg/s	Injected fuel flow
W_t	kg/s	Mass flow through the turbine
x_{EGR}	%	Amount of EGR in the intake manifold
λ	-	Air-to-fuel equivalence ratio
ω_t	rad/s	Turbocharger speed

References

[1] T. Glad and L. Ljung. *Reglerteknik*. Studentlitteratur, 1989.

[2] T. Glad and L. Ljung. *Reglerteori*. Studentlitteratur, second edition, 2003.

[3] M. van Nieuwstadt I. Kolmanovsky, P. Moraal and A.G. Stefanopoulou. Issues in modelling and cotrol of intake flow in variable geometry turbocharged engines.

[4] L. Nielsen and L. Eriksson. *Course material Vehicular Systems*. Bokakademin, Linköping University, Linköping, Sweden, 2004.

[5] A. Persson and L-Ch. Böiers. *Analys i flera variabler*. Studentlitteratur, second edition, 2003.

[6] P. Skogtjärn. Modelling of the exhaust gas temperature for diesel engines. Master's thesis LiTH-ISY-EX-3379, Department of Electrical Engineering, Linköpings Universitet, Linköping, Sweden, December 2002.

[7] J. Wahlström. Modeling of a diesel engine with vgt and egr. Technical report, Division of Vehicular Systems, Linköping University, Linköping, Sweden, 2005.